The 9th European Congress on Computational Methods in Applied Sciences and Engineering
ECCOMAS Congress 2024
3 – 7 June 2024, Lisboa, Portugal

VIBRATION ANALYSIS OF FGM SANDWICH PANEL WITH CUT-OUTS USING REFINED HSDT BASED ON ISOGEOMETRIC ANALYSIS

LOKANATH BARIK*, ABINASH KUMAR SWAIN†

* Mechanical and Industrial Engineering (MIED)
Indian Institute of Technology Roorkee
Roorkee, 247667 Uttarakhand, India
e-mail: lokanath_b@me.iitr.ac.in

† Mechanical and Industrial Engineering (MIED)
Indian Institute of Technology Roorkee
Roorkee, 247667 Uttarakhand, India
e-mail: abinash.swain@me.iitr.ac.in

Keywords: Isogeometric analysis, Multipatch coupling, FGM sandwich structure, Refined HSDT, Vibration analysis.

Summary. This paper presents the applicability of a novel strong coupling methodology in maintaining continuity across adjacent patch interfaces in multi-patch isogeometric analysis. FGM sandwich plate is modelled using refined higher-order shear deformation theory, and the present IGA formulation is validated with past literature on FGM hardcore and softcore arrangement. The free vibration analysis of the FGM plate having multi-patch geometries is conducted to test the accuracy of the proposed coupling. The results show the optimal accuracy and effectiveness of the coupling algorithm to enforce continuity across arbitrarily shaped patches for vibration analysis of FGM sandwich structure with cutouts.

1 INTRODUCTION

The FGM sandwich structure has received much attention due to its lightweight design and tailored mechanical properties. The distinctive characteristics of these plates are extensively researched, particularly relating to load-bearing constructions that require specific stiffness, thermal resistance, and strength distribution across their thickness [1]. These structures are generally considered for aerospace, aircraft, and defence applications, where vibration analysis, a crucial factor in designing, plays a significant role in ensuring their structural integrity and performance [2]. Hadji et al. [3] performed free vibration analysis on FGM-based sandwich plates using four variable-based refined plate theory (RPT). The equation of motion was derived using the Hamilton principle and solved by Navier's technique. The validation and accuracy were compared with other plate theories. Thai et al. [4] performed an HSDT analysis of FGM-based sandwich plates under thermo-mechanical loading. The governing equation was derived from the Galerkin form and solved numerically using IGA. Liu et al. [5] studied free vibration analysis of FGM sandwich structure with both face sheets and core made of being functionally graded following a power law function. Van et al. [6] performed an isogeometric analysis of a

multi-layer FGM structure with graphene-reinforced platelets on composite nanoplates. IGA was proven effective in solving the kinetic equations and subsequent analysis of graphene microbeams.

Holes and intrinsic profiles significantly affect the natural frequencies compared to monolithic plates. Hence, understanding the vibration characteristics of sandwich structures with cutouts is vital. In IGA, these structures are modelled using multi-patch geometries that break the C1 continuity near the adjoining patch junction. To resolve this issue, researchers developed patch coupling techniques for solving the higher-order PDE [7]. Wang et al. studied geometries with arbitrary-shaped cutouts for conducting free vibration analysis of stiffened plates using IGA-based HSDT formulation and Nitche method. In [8], they extended their work to stiffened composite plates and studied the natural frequency responses for different fibre orientations, angles, shapes and sizes using IGA and HSDT. Devarajan and Kapania [9] investigated multi-patch composite structures and used the Nitche method to predict the critical thermal buckling load on composite structures. He et al. [10] used the Nitche method to investigate the thermal behaviour of arbitrarily shaped complex plates using IGA and adaptive refinement strategies. However, the Nitche method needs additional stabilisation parameters to weakly enforce continuity along the patch boundary. However, strong coupling methods enforce continuity by generating approximate basis functions that are continuous over the patch junction edge and throughout the domain without any additional conditioning in the weak form. Its effectiveness in the topology optimisation of plates is discussed in [11] for multi-patch geometries and efficient patch coupling. However, vibration analysis of FGM sandwich structure using such strong coupling methodologies is absent in the literature.

This paper presents a novel application of the strong coupling methodology proposed by [12] to model complex FGM sandwich structures with multi-patch geometries using refined HSDT formulation. Frequency responses of sandwich plates with circular holes and arbitrary patches are studied, and the effectiveness of the coupling algorithm is demonstrated.

2 REFINED HSDT FORMULATION FOR FGM SANDWICH STRUCTURE

Let us consider a sandwich panel with three layers of plate structure, as shown in Fig. 1, where the top and bottom face plates are made of FGM material, and the core has a homogenous property distribution. The FGM plates gradually vary in geometrical properties from ceramic to metal or vice versa based on the core configuration along the thickness. The softcore arrangement has a metallic core, and hence, the FGM properties vary from ceramic to metal from the face surface to the inner region. Contrary to this, the core is made of ceramic material in a hardcore arrangement, and the FGM properties vary from metal to ceramic. The variation of Young's modulus and density of the FGM plates for both core arrangements is given by,

Hardcore:

$$X(z) = X_m + \left(X_c - X_m\right)\left(\frac{h - h_0}{h_1 - h_0}\right)^n \qquad h_0 \le h \le h_1$$

$$X(z) = X_c \qquad h_1 \le h \le h_2$$

$$X(z) = X_m + \left(X_c - X_m\right)\left(\frac{h-h_3}{h_2-h_3}\right)^n \qquad h_2 \le h \le h_3$$

Softcore:

$$X(z) = X_c + \left(X_m - X_c\right)\left(\frac{h-h_0}{h_1-h_0}\right)^n \qquad h_0 \le h \le h_1$$

$$X(z) = X_m \qquad h_1 \le h \le h_2$$

$$X(z) = X_c + \left(X_m - X_c\right)\left(\frac{h-h_3}{h_2-h_3}\right)^n \qquad h_2 \le h \le h_3$$

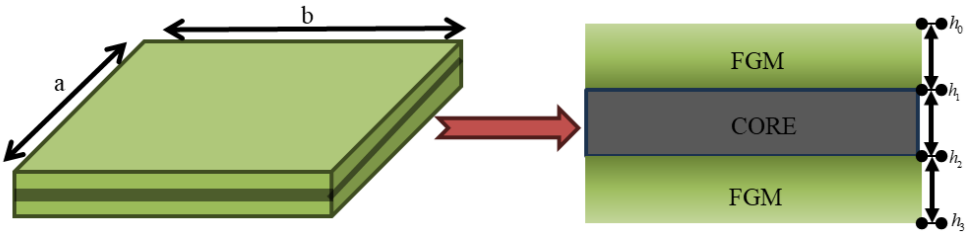

Figure 1: FGM sandwich structure layer-wise distribution with homogenous core.

4.1 Refined HSDT and Equation of motion

To determine the displacement field, refined higher order shear deformation theory is used without considering any shear correction factor

$$\begin{aligned} u(x,y,z) &= u_0 - zw_{b,x} + g(z)w_{s,x} \\ v(x,y,z) &= v_0 - zw_{b,y} + g(z)w_{s,y} \\ w(x,y,z) &= w_b + w_s \end{aligned} \tag{1}$$

u_0, v_0: denotes in-plane displacement along the x and y directions

w_b, w_s: component of bending and shear of transverse displacement

The linear strain of the displacement field expressed by Von-Kerman principle as:

$$\{\varepsilon\} = \begin{Bmatrix} \varepsilon_{xx} \\ \varepsilon_{yy} \\ \gamma_{xy} \\ \gamma_{xz} \\ \gamma_{yz} \end{Bmatrix} = \begin{Bmatrix} \varepsilon_0 + z\varepsilon_1 + g(z)\varepsilon_2 \\ 1 + g'(z)\varepsilon_s \end{Bmatrix} \tag{2}$$

Where,

$$\varepsilon_0 = \begin{Bmatrix} u_{0,x} \\ v_{0,y} \\ u_{0,y} + v_{0,x} \end{Bmatrix}, \quad \varepsilon_1 = -\begin{Bmatrix} w_{b,xx} \\ w_{b,yy} \\ 2w_{b,xy} \end{Bmatrix}, \quad \varepsilon_2 = \begin{Bmatrix} w_{s,xx} \\ w_{s,yy} \\ 2w_{s,xy} \end{Bmatrix}, \quad \varepsilon_s = \begin{Bmatrix} w_{s,x} \\ w_{s,y} \end{Bmatrix}$$

The constitutive relation between stress and strain field from Hook's law can be written as

$$\begin{Bmatrix} \sigma_{xx} \\ \sigma_{yy} \\ \tau_{xy} \\ \tau_{xz} \\ \tau_{yz} \end{Bmatrix} = \begin{bmatrix} Q_{11} & Q_{12} & 0 & 0 & 0 \\ Q_{12} & Q_{22} & 0 & 0 & 0 \\ 0 & 0 & Q_{66} & 0 & 0 \\ 0 & 0 & 0 & Q_{55} & 0 \\ 0 & 0 & 0 & 0 & Q_{44} \end{bmatrix} \begin{Bmatrix} \varepsilon_{xx} \\ \varepsilon_{yy} \\ \gamma_{xy} \\ \gamma_{xz} \\ \gamma_{yz} \end{Bmatrix} \tag{3}$$

Stiffness coefficients are defined accordingly

$$Q_{11} = Q_{22} = \frac{E(z)}{1-\mu^2}, \quad Q_{12} = Q_{21} = \frac{\mu E(z)}{1-\mu^2}, \quad Q_{44} = Q_{55} = Q_{66} = \frac{E(z)}{2(1+\mu)}$$

The governing equation for equilibrium derived from the Hamilton's principle as

$$\int_0^t (\delta \prod + \delta V - \delta K) dt = 0 \tag{4}$$

Where the virtual strain energy defined as

$$\delta \prod = \int_v \delta \varepsilon^T \sigma dV \tag{5}$$

Substituting equation (3) into equation (5), the virtual strain energy written in the form of

$$\delta \prod = \int_\Omega \delta \varepsilon^T D \varepsilon d\Omega$$

Where,

$$D = \begin{bmatrix} A & B & D & 0 \\ B & E & F & 0 \\ D & F & H & 0 \\ 0 & 0 & 0 & D^s \end{bmatrix}$$

$$(A, B, D, E, F, H) = \int_{-h/2}^{h/2} Q_{ij} (1, z, f(z), z^2, zf(z), f(z)^2) dz$$

$$D^s = \int_{-h/2}^{h/2} Q_{ij} (1 + g'(z))^2$$

The general form of strain vector defined in the form of

$$\bar{\varepsilon} = \{ \varepsilon_0 \quad \varepsilon_1 \quad \varepsilon_2 \quad \varepsilon_s \}^T$$

Both potential energy and kinetic energy defined in equation (6) and (7) respectively

$$\delta V = \int_\Omega q \delta (w_b + w_s) \, d\Omega \tag{6}$$

$$\delta K = \int \delta \dot{u}^T \rho(z)\, \dot{u} dv \tag{7}$$

For determining the kinetic energy, vector *u* defined from the displacement field

$$u = \begin{Bmatrix} u \\ v \\ w \end{Bmatrix} = u_0 + z u_1 + g(z) u_2 \tag{8}$$

$$u_0 = \begin{Bmatrix} u_0 \\ v_0 \\ w_b + w_w \end{Bmatrix}, \quad u_1 = -\begin{Bmatrix} w_{b,x} \\ w_{b,y} \\ 0 \end{Bmatrix}, \quad u_1 = -\begin{Bmatrix} w_{s,x} \\ w_{s,y} \\ 0 \end{Bmatrix}$$

$$\int_0^t (\delta K) dt = -\int_0^t \left[\int_V \left(\delta \ddot{u} \rho(z) u \right) dV \right] dt$$

Substituting equation (8) in equation (7)

$$\delta K = -\int_\Omega \delta \bar{\ddot{u}}^T m \bar{\ddot{u}} d\Omega$$

where

$$\bar{u} = \{u_0 \; u_1 \; u_2\}^T$$

And m is the mass matrix

$$m = \begin{bmatrix} I_0 & 0 & 0 \\ 0 & I_0 & 0 \\ 0 & 0 & I_0 \end{bmatrix}, \text{ where } \; I_0 = \begin{bmatrix} I_1 & I_2 & I_4 \\ I_2 & I_3 & I_5 \\ I_4 & I_5 & I_6 \end{bmatrix}$$

$$. (I_1, I_2, I_3, I_4, I_5, I_6) = \int_{\frac{-h}{2}}^{\frac{h}{2}} \rho(z)(1, z, z^2, f(z), z f(z), f(z)^2) dz \; .$$

By combining above equations of different energy, the Hamilton equilibrium principle rewritten in the form as given

$$\int_\Omega \delta \bar{\varepsilon}^T D \bar{\varepsilon} d\Omega + \int_\Omega \delta \bar{\ddot{u}}^T m \bar{\ddot{u}} d\Omega = \int_\Omega q \delta (w_b + w_s) d\Omega \tag{9}$$

3 MULTIPATCH COUPLING AND IGA FORMULATION

The NURBS basis functions are C^1 continuous within the defined domain of knot vectors. In multi-patch geometries, where two or more patches intersect, C^0 continuity is observed. The basis functions responsible for discontinuity near the junction are removed, and a new set of C^1 smooth isogeometric functions are developed using a linear combination of these pre-existing C^0 bases following the approach of [12]. These modified bases are further used for NURBS-based discretization and solving the equation of motion. Based on 2-D NURBS basis functions, the displacement considered is as follows

$$u^h(\eta,\zeta)=\sum_{e=1}^{n\times m}N_e(\eta,\zeta)d_e$$

Where N_e is the modified NURBS shape function

$$N_e(\eta,\zeta)=\begin{bmatrix}N_e(\eta,\zeta) & 0 & 0 & 0\\ 0 & N_e(\eta,\zeta) & 0 & 0\\ 0 & 0 & N_e(\eta,\zeta) & 0\\ 0 & 0 & 0 & N_e(\eta,\zeta)\end{bmatrix};\ d_e=\{u_{0e}\ v_{0e}\ w_{be}\ w_{se}\}^T$$

The strain fields can be written as,

$$\bar{\varepsilon}=\sum_{e=1}^{n\times m}\left[B_{0e}\ \mathrm{B}_{1e}\ \mathrm{B}_{2e}\ \mathrm{B}_{se}\right]^T d_e \tag{10}$$

$$B_{0e}=\begin{bmatrix}N_{e,x} & 0 & 0 & 0\\ 0 & N_{e,y} & 0 & 0\\ N_{e,y} & N_{e,x} & 0 & 0\end{bmatrix},\ B_{1e}=-\begin{bmatrix}0 & 0 & N_{e,xx} & 0\\ 0 & 0 & N_{e,yy} & 0\\ 0 & 0 & 2N_{e,xy} & 0\end{bmatrix},\ B_{2e}=\begin{bmatrix}0 & 0 & 0 & N_{e,xx}\\ 0 & 0 & 0 & N_{e,yy}\\ 0 & 0 & 0 & 2N_{e,xy}\end{bmatrix},$$

$$B_{se}=\begin{bmatrix}0 & 0 & 0 & N_{e,x}\\ 0 & 0 & 0 & N_{e,y}\end{bmatrix}$$

Substituting equation (10) in governing equation (9) we get

$$Kd+M\ddot{d}=f \tag{11}$$

Where *K* is the stiffness $K=\int_\Omega B^T DB d\Omega$ and *M* is the mass matrix $M=\int_\Omega \bar{N}^T m\bar{N}d\Omega$.

$$\bar{N}=\begin{bmatrix}N_e & 0 & 0 & 0 & 0 & 0 & -N_{e,x} & 0 & 0 & 0 & 0 & N_{e,x}\\ 0 & N_e & 0 & 0 & 0 & 0 & -N_{e,y} & 0 & 0 & 0 & 0 & N_{e,y}\\ 0 & 0 & N_e & N_e & 0 & 0 & 0 & 0 & 0 & 0 & 0 & 0\end{bmatrix}$$

And *f* is the force vector expressed as

$$f=\int_\Omega\{0\ \ 0\ \ N_e\ \ N_e\}^T q d\Omega$$

Free vibration considered without external force vector is rewritten as

$$Kd+M\ddot{d}=0 \tag{12}$$

$$d(x,t)=D_0(x)e^{i\omega t} \tag{13}$$

$$(K-\omega^2 M)d=0 \tag{14}$$

$$(K-\omega^2 M)d=0$$

Where d is the nonzero displacement and ω is the natural frequency.

4 RESULTS AND DISCUSSIONS

In this section, we discuss the results obtained from the FGM sandwich plate with softcore and hardcore arrangements. The sandwich plate comprises Aluminum (Al) having metallic constituents and Alumina (Al_2O_3) as the ceramic part, having mechanical properties

$E_m = 70$ GPa, $\rho_m = 2707$ Kg/m^3, $\upsilon_m = 0.3$ and $E_c = 380$ GPa, $\rho_c = 3800$ Kg/m^3, $\upsilon_c = 0.3$ respectively. The boundary conditions (B.C) are applied to the outer boundary of the sandwich plate, which is mainly simply supported (SSSS) and clamped (CCCC) types. Numerical results are obtained using modified C^1 coupled basis functions in multi-patch geometry formulation. Based on the approximations, $(p+1)\times(q+1)$ gauss points are selected for integration over 2D domains. The B.Cs influence over the degrees of freedom are given by,

Simply supported (SSSS):

$$\begin{aligned} v_0 = w_b = w_s = 0 \ at \ x = 0, a \\ u_0 = w_b = w_s = 0 \ at \ y = 0, b \end{aligned} \tag{15}$$

Clamped (CCCC):

$$u_0 = v_0 = w_b = w_s = w_{b,n} = w_{s,n} = 0 \tag{16}$$

4.1 Validation of FGM sandwich plate

Numerical validation of the proposed NURBS-based refined HSDT model with IGA multi-patch algorithm is presented in this section. FGM sandwich square plate of unit length with SSSS and CCCC boundary conditions is shown in Table 1 and Table 2 for softcore and hardcore arrangement, respectively. The sandwich plate is divided into two patches, as shown in Fig. 2, along the x-axis, where the dotted line represents the patch boundary. Dimensionless natural frequency is presented such that $\omega = \omega a^2 / h.\sqrt{\rho_0 / E_0}$, where $\rho_0 = 1$ Kg/m^3 and $E_0 = 1$ GPa. The results show that the two patch results match well with the results from [2] for various sandwich configurations and the thickness-to-width ratio of the square plate.

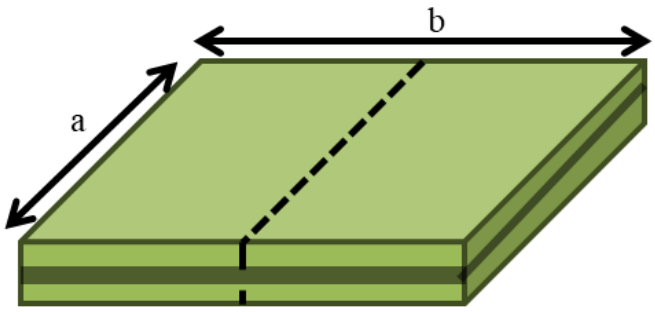

Figure 2: Illustration of a two-patch FGM sandwich plate.

Table 1: FGM sandwich square plate first dimensionless natural frequency for softcore arrangement.

B.C	n	Methodology	1-0-1	2-1-2	2-1-1	1-1-1	2-2-1	1-2-1
SSSS	0.5	Li et al. [2]	1.5735	1.5258	1.4846	1.4341	1.4166	1.2055
		Two patch	1.5750	1.5289	1.4866	1.4362	1.4162	1.2048
	1	Li et al. [2]	1.7223	1.6744	1.6305	1.5704	1.5579	1.3083
		Two patch	1.7257	1.6838	1.6396	1.5789	1.5610	1.3076
	5	Li et al. [2]	1.8420	1.8261	1.7896	1.7273	1.7267	1.4665
		Two patch	1.8420	1.8416	1.8173	1.7534	1.7486	1.4660

B.C	n	Methodology	1-0-1	2-1-2	2-1-1	1-1-1	2-2-1	1-2-1
SSSS	0.5	Li et al. [2]	1.5735	1.5258	1.4846	1.4341	1.4166	1.2055
		Two patch	1.5750	1.5289	1.4866	1.4362	1.4162	1.2048
	10	Li et al. [2]	1.8402	1.8399	1.8081	1.7478	1.7481	1.4948
		Two patch	1.8386	1.8520	1.8366	1.7755	1.7758	1.4943
CCCC	0.5	Li et al. [2]	2.5985	2.4933	2.4182	2.3497	2.3127	2.0112
		Two patch	2.6302	2.5313	2.4521	2.3830	2.3363	2.0285
	1	Li et al. [2]	2.8445	2.7121	2.6191	2.5396	2.5011	2.1548
		Two patch	2.8864	2.7772	2.6824	2.6007	2.5413	2.1765
	5	Li et al. [2]	3.1144	2.9873	2.8560	2.7715	2.7156	2.3649
		Two patch	3.1404	3.0788	2.9910	2.9015	2.8262	2.3924
	10	Li et al. [2]	3.1363	3.0368	2.8995	2.8140	2.7452	2.4016
		Two patch	3.1535	3.1150	3.0385	2.9505	2.8769	2.4299

Table 2: FGM sandwich square plate first dimensionless natural frequency for hardcore arrangement.

B.C	n	Methodology	1-0-1	2-1-2	2-1-1	1-1-1	2-2-1	1-2-1
SSSS	0.5	Li et al. [2]	1.4461	1.4861	1.5213	1.5493	1.5767	1.7113
		Two patch	1.4442	1.4841	1.5192	1.5471	1.5745	1.7090
	1	Li et al. [2]	1.2447	1.3018	1.3552	1.3976	1.4414	1.6511
		Two patch	1.2432	1.3001	1.3533	1.3957	1.4393	1.6489
	5	Li et al. [2]	0.9448	0.9810	1.0453	1.1098	1.1757	1.5299
		Two patch	0.9460	0.9818	1.0447	1.1090	1.1740	1.5279
	10	Li et al. [2]	0.9273	0.9408	0.9952	1.0610	1.1247	1.5033
		Two patch	0.9284	0.9430	0.9955	1.0611	1.1231	1.5014
CCCC	0.5	Li et al. [2]	2.5259	2.5949	2.6536	2.6983	2.7499	2.9584
		Two patch	2.5313	2.6003	2.6592	2.7048	2.7501	2.9667
	1	Li et al. [2]	2.1902	2.2911	2.3819	2.4511	2.5398	2.8626
		Two patch	2.1934	2.2937	2.3843	2.4551	2.5280	2.8696
	5	Li et al. [2]	1.66187	1.7393	1.8579	1.9672	2.1572	2.6674
		Two patch	1.6763	1.7499	1.8609	1.9726	2.0831	2.6724
	10	Li et al. [2]	1.6212	1.6633	1.7686	1.8808	1.9986	2.6243
		Two patch	1.6362	1.6813	1.7760	1.8905	1.9966	2.6289

With the increase in power law exponent, the natural frequency rises for softcore arrangement, and it decreases in the case of hardcore arrangement of FGM sandwich structure for both boundary conditions. The results of the two-patch sandwich plate geometry are in excellent agreement with the literature. Hence, the given strong coupling method is highly accurate in maintaining continuity between patches and hence can be used in further analysis.

4.2 Analysis of multi-patch circular plate

In this example, a circular FGM sandwich plate has five patches, as shown in Fig. 3. The patches are separated by patch boundaries represented in dotted lines, and the circle is enforced with CCCC boundary conditions around the outer periphery. The radius is considered as $r = 0.5$

and $h/r = 0.2$. Table 3 represents the dimensionless frequencies $\omega = \omega r^2 / h.\sqrt{\rho_0 / E_0}$, for three sandwich configurations, 1-1-1, 2-1-1, and 1-2-1, with variable power law index. The fundamental natural frequencies of the plate with both softcore and hardcore configurations are noted.

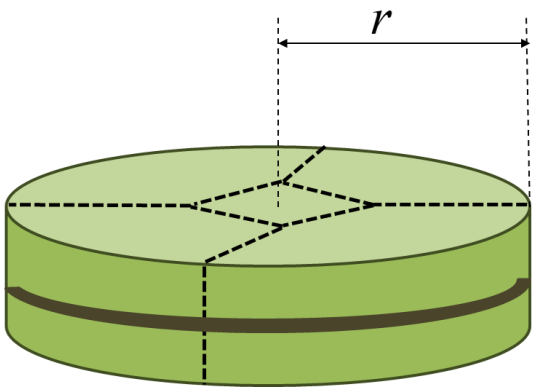

Figure 3: Five-patch circular sandwich plate geometry

Table 3: First dimensionless natural frequency of clamped FGM circular sandwich plate.

Arrangement	n	1-0-1	2-1-2	2-1-1	1-1-1	2-2-1	1-2-1
Softcore	0.5	0.8605	0.8397	0.8183	0.7883	0.7795	0.6550
	1	0.9420	0.9270	0.9073	0.8707	0.8664	0.7158
	5	0.9944	1.0057	1.0019	0.9642	0.9752	0.8123
	10	0.9891	1.0077	1.0093	0.9737	0.9889	0.8299
Hardcore	0.5	0.7677	0.7890	0.8081	0.8237	0.8385	0.9132
	1	0.6586	0.6887	0.7174	0.7409	0.7642	0.8798
	5	0.5002	0.5175	0.5507	0.5864	0.6200	0.8130
	10	0.4922	0.4969	0.5244	0.5609	0.5926	0.7984

Similar trends in frequency responses are obtained for circular geometry with arbitrary patches for softcore and hardcore arrangement, as stated in section 4.1.

4.3 Analysis of annular plate

An annular FGM sandwich plate is shown in Fig. 4 with a circular cut-out of radius 0.2. The plate is divided into four patches separated by adjacent patch junction edges. The fundamental dimensionless natural frequency value $\omega = \omega(r_0^2 - r_i^2) / h.\sqrt{\rho_0 / E_0}$ for the annular sandwich plate with hardcore and softcore arrangement is shown in Table 4. The plate is fully clamped at the outer periphery and free at the inner boundary. The effect of varying power law index on the natural frequency of the plate is studied with $h / r_0 = 0.2$.

0.8814	0.9042	0.9207	0.9315	0.9435	0.9926
0.7868	0.8225	0.8497	0.8683	0.8882	0.9697
0.6109	0.6504	0.6906	0.7291	0.7628	0.9218
0.5841	0.6257	0.6624	0.7028	0.7357	0.9112

Figure 4: Annular sandwich plate with four patches.

Table 3: First dimensionless natural frequency of clamped FGM annular sandwich plate.

Arrangement	n	1-0-1	2-1-2	2-1-1	1-1-1	2-2-1	1-2-1
Softcore	0.5	0.7744	0.7279	0.6982	0.6890	0.6655	0.6118
	1	0.8534	0.7908	0.7484	0.7376	0.7008	0.6350
	5	0.9847	0.9090	0.8470	0.8325	0.7665	0.6633
	10	1.0093	0.9360	0.8719	0.8562	0.7844	0.6679
Hardcore	0.5	0.8814	0.9042	0.9207	0.9315	0.9435	0.9926
	1	0.7868	0.8225	0.8497	0.8683	0.8882	0.9697
	5	0.6109	0.6504	0.6906	0.7291	0.7628	0.9218
	10	0.5841	0.6257	0.6624	0.7028	0.7357	0.9112

5 CONCLUSIONS

This paper presents a novel application of the strong coupling method to find the vibration response of the FGM sandwich structure governed by refined HSDT formulation. The refined theory reduces the degrees of freedom, making the numerical analysis computationally more efficient. The coupling results match the literature on FGM sandwich structure with hardcore and softcore arrangements and clamped and supported boundary conditions. Hence, a promising coupling method for analyzing sandwich plates with various configurations has been established. The frequency results from multi-patch circular and annular plates show similar trends to square plate geometry. The given analysis clearly shows the effect of cutouts and geometry changes on the natural frequency of plates. Hence, it serves as a benchmark for the efficient design and production of FGM sandwich plates. The following work can be further extended to investigate different types of plates and shells with cutouts. More complex geometrical structures can also be analyzed for thermal buckling and vibration responses.

REFERENCES

[1] A. Garg, M. O. Belarbi, H. D. Chalak, and A. Chakrabarti, “A review of the analysis of sandwich FGM structures,” *Compos. Struct.*, vol. 258, no. October 2020, p. 113427, 2021, doi: 10.1016/j.compstruct.2020.113427.

[2] Q. Li, V. P. Iu, and K. P. Kou, “Three-dimensional vibration analysis of functionally graded material sandwich plates,” *J. Sound Vib.*, vol. 311, no. 1–2, pp. 498–515, 2008, doi: 10.1016/j.jsv.2007.09.018.

[3] L. Hadji, H. A. Atmane, A. Tounsi, I. Mechab, and E. A. Adda Bedia, “Free vibration of functionally graded sandwich plates using four-variable refined plate theory,” *Appl. Math. Mech. (English Ed.*, vol. 32, no. 7, pp. 925–942, 2011, doi: 10.1007/s10483-011-1470-9.

[4] C. H. Thai, A. M. Zenkour, M. Abdel Wahab, and H. Nguyen-Xuan, “A simple four-unknown shear and normal deformations theory for functionally graded isotropic and sandwich plates based on isogeometric analysis,” *Compos. Struct.*, vol. 139, pp. 77–95,

2016, doi: 10.1016/j.compstruct.2015.11.066.
[5] M. Liu, Y. Cheng, and J. Liu, “High-order free vibration analysis of sandwich plates with both functionally graded face sheets and functionally graded flexible core,” *Compos. Part B Eng.*, vol. 72, pp. 97–107, 2015, doi: 10.1016/j.compositesb.2014.11.037.
[6] P. Phung-Van, Q. X. Lieu, A. J. M. Ferreira, and C. H. Thai, “A refined nonlocal isogeometric model for multilayer functionally graded graphene platelet-reinforced composite nanoplates,” *Thin-Walled Struct.*, vol. 164, no. November 2020, p. 107862, 2021, doi: 10.1016/j.tws.2021.107862.
[7] Y. Wang, J. Fan, X. Shen, X. Liu, J. Zhang, and N. Ren, “Free vibration analysis of stiffened rectangular plate with cutouts using Nitsche based IGA method,” *Thin-Walled Struct.*, vol. 181, no. December 2021, p. 109975, 2022, doi: 10.1016/j.tws.2022.109975.
[8] Y. Wang *et al.*, “Nitsche-based isogeometric approach for free vibration analysis of laminated plate with multiple stiffeners and cutouts,” *Int. J. Mech. Sci.*, vol. 244, no. October 2022, p. 108041, 2023, doi: 10.1016/j.ijmecsci.2022.108041.
[9] B. Devarajan and R. K. Kapania, “Thermal buckling of curvilinearly stiffened laminated composite plates with cutouts using isogeometric analysis,” *Compos. Struct.*, vol. 238, no. November 2019, p. 111881, 2020, doi: 10.1016/j.compstruct.2020.111881.
[10] Q. He, T. Yu, L. Van Lich, and T. Q. Bui, “Thermal buckling adaptive multi-patch isogeometric analysis of arbitrary complex-shaped plates based on locally refined NURBS and Nitsche’s method,” *Thin-Walled Struct.*, vol. 169, no. September, p. 108383, 2021, doi: 10.1016/j.tws.2021.108383.
[11] P. L. Karuthedath, L. Barik, A. Gupta, A. K. Swain, R. Chowdhury, and B. Mamindlapelly, “A C1 continuous multi-patch framework for adaptive isogeometric topology optimization of plate structures,” *Comput. Methods Appl. Mech. Eng.*, vol. 429, no. May, p. 117132, 2024, doi: 10.1016/j.cma.2024.117132.
[12] C. L. Chan, C. Anitescu, and T. Rabczuk, “Strong multipatch C1-coupling for isogeometric analysis on 2D and 3D domains,” *Comput. Methods Appl. Mech. Eng.*, vol. 357, 2019, doi: 10.1016/j.cma.2019.112599.